Locally Conformal Cell for Two-Dimensional TLM

Poman P.M. So and Wolfgang J.R. Hoefer

Computational Electromagnetics Research Laboratory
Department of Electrical and Computer Engineering
University of Victoria
Victoria, BC, V8W 3P6, Canada

ABSTRACT — We propose a locally conformal TLM cell that requires no change in the scattering algorithm and eliminates the time step constraint imposed by graded meshing. It also circumvents the need for time and space interpolations required by multi- and sub-gridding schemes. Simulation results confirm the accuracy and versatility of the approach.

Keywords — Time Domain Modeling, TLM method, mesh refinement, mesh generation.

I. INTRODUCTION

Irregular meshing has been an important issue for time-domain based field solvers. It has been used to model curved and moving boundaries [1,2]. To avoid graded meshing which imposes the stable time step in the smallest cell upon the entire mesh, methods based on multi-gridding or sub-gridding [3–8] as well as hybrid methods [9] have been developed. However, they require interpolation in space and time that may cause errors and even instability. We have developed a local mesh modification method that is not subject to the minimal time-step constraint, requires no averaging and no change in the scattering algorithm. Rather, a change in the size and shape of a TLM cell due to an irregular boundary position is translated into a change in its input impedance at the cell interfaces with the regular computational mesh.

The locally conformal cell is a square TLM cell with a regular impulse scattering matrix and a regular transit time, but its link line impedances are transformed in such a way that it has the characteristics of a fraction of a regular square cell — a fractional cell. To connect such a fractional cell to a regular cell, a scattering procedure must be introduced at the interface between them; the same applies to the connection between two different conformal cells. The scattering procedure is equivalent to the insertion of an ideal transformer between cells.

FRACTIONAL CELL WITH AN ELECTRIC WALL

Figure 1a shows a parallel plate waveguide consisting of a chain of regular square 2D TLM shunt cells terminated by an electric wall at a distance from the last regular cell which is a fraction of the cell size. Figure 1b shows an electrically identical situation in which the fractional cell has been replaced by a cell of standard size. The properties of the latter cell must be such that the impedance seen when looking to the right at the interface is the same in both cases.

The input impedances of the fractional cell and the standard-size cell at the interface are Z_{ir} and Z_{ia}, respectively, where:

$$Z_{ir} = jZ_r \tan(\beta_r \delta) \approx jZ_r \beta_r \delta \tag{1}$$

$$Z_{ia} = jZ_a \tan(\beta_a \Delta l) \approx jZ_a \beta_a \Delta l \tag{2}$$

For equivalence of the two cases, Z_{ir} and Z_{ia} must be identical. In terms of the characteristics of the cells shown in Figure 2, the quantities in Eq 1 and Eq 2 are:

$$\begin{aligned} Z_r &= \sqrt{L_o / 2C_o}, & \beta_r &= \omega\sqrt{2L_oC_o} \\ Z_a &= \sqrt{L_x /(C_x + C_y)}, & \beta_a &= \omega\sqrt{L_x(C_x + C_y)} \end{aligned} \tag{3}$$

where L_o, C_o, L_x, C_x, L_y, and C_y are the inductances and capacitances per unit length of the link lines. Introducing Eq 3 into Eq 1 and Eq 2 and equating the two impedances yields:

$$\sqrt{\frac{L_o}{2C_o}}\omega\sqrt{2L_oC_o} = \sqrt{\frac{L_x}{C_x + C_y}}\omega\sqrt{L_x(C_x + C_y)\Delta l} \tag{4}$$

which can be simplified to give:

$$L_x = L_o \frac{\delta}{\Delta l} \tag{5}$$

Conservation of the scattering matrix and of the transit time of the standard-size cell requires that the link line impedances and the link line speeds must be the same in x- and y-directions, i.e.:

0-7803-7695-1/03/$17.00 © 2003 IEEE

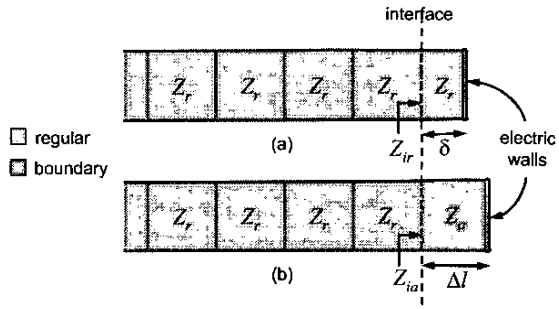

Figure 1 The equivalence between a fraction of the regular TLM cell (fractional cell) and the standard-size boundary cell; both are terminated by electric walls.

$$\sqrt{\frac{L_x}{C_x}} = \sqrt{\frac{L_y}{C_y}} \quad \text{and} \quad \sqrt{L_x C_x} = \sqrt{L_y C_y} \tag{6}$$

This requires:

$$L_x = L_y \quad \text{and} \quad C_x = C_y \tag{7}$$

Finally, since the transit time for the fractional cell must be the same as that of a standard-size boundary cell, i.e.:

$$\sqrt{L_o C_o} = \sqrt{L_x C_x} \tag{8}$$

Combining Eq 5 and 8 yields:

$$C_x = C_o \frac{L_o}{L_x} = C_o \frac{\Delta l}{\delta} = C_y \tag{9}$$

Thus the properties of the short-circuited boundary cell for any deformation ratio, $\delta / \Delta l$, are:

$$\begin{aligned} Z_x = Z_y &= \sqrt{\frac{L_x}{C_x}} = \sqrt{\frac{L_y}{C_y}} = Z_o \frac{\delta}{\Delta l} \\ Z_a &= \sqrt{\frac{L_x}{2C_x}} = Z_r \frac{\delta}{\Delta l} \end{aligned} \tag{10}$$

Connection of this cell to the regular mesh requires the introduction of the following scattering procedure at the interface:

$$\begin{bmatrix} B_i \\ B_{i+1} \end{bmatrix} = \begin{bmatrix} \frac{n-1}{n+1} & \frac{2}{n+1} \\ \frac{2n}{n+1} & \frac{n-1}{n+1} \end{bmatrix} \begin{bmatrix} A_i \\ A_{i+1} \end{bmatrix} \tag{11}$$

where $n = \delta / \Delta l$ can be smaller or larger than 1, and the definition of A and B are given in Figure 3.

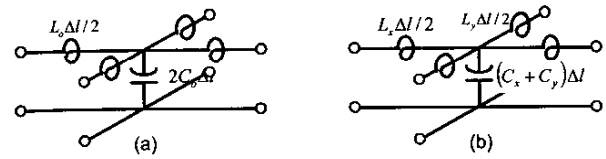

Figure 2 The equivalence of the regular cell and the boundary cell. (a) A regular cell with two link lines of $Z_o = \sqrt{L_o / C_o}$. (b) A boundary cell with two link lines of $Z_x = \sqrt{L_x / C_x}$ and $Z_y = \sqrt{L_y / C_y}$.

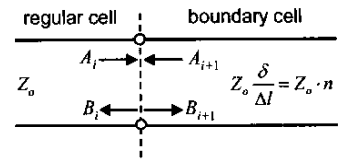

Figure 3 Connection of a regular cell to a boundary cell.

FRACTIONAL CELL WITH TWO ELECTRIC WALLS

The conformal boundary cell theory derived in the previous section can be applied to the connection between adjacent boundary cells; this allows a fractional cell terminated on two adjacent sides by electric walls to be modeled by a boundary cell; Figure 4a shows the equivalence between a fractional cell bounded by two electric walls at some arbitrary positions, and a boundary cell bounded by two electric walls at the regular positions. Figure 4b shows the successive applications of the conformal boundary cell theory, first by assuming that the fractional cell has been shortened only along one direction, and then by shortening the resulting boundary cell again in the other direction; and the result is:

$$Z_a = Z_r \frac{\delta_x \delta_y}{\Delta l \Delta l} \tag{12}$$

That means, Eq 11 must be applied to the interfaces between regions with Z_r and Z_a. In this situation, $n = \delta_x \delta_y / (\Delta l \Delta l)$.

BOUNDARY-CONFORMAL MESH

Whenever a boundary is not located exactly halfway between two nodes, conformal boundary cells can be used to replace the fractional regular cells that are affected by the boundary, Figure 5a depicts such a situation. Replacing the regular cells affected by the boundary in a TLM mesh with the boundary cells of the appropriate impedance values produces a TLM mesh with cells having the centers electrically displaced from their original positions (Figure 5c); this yield a locally conformal mesh.

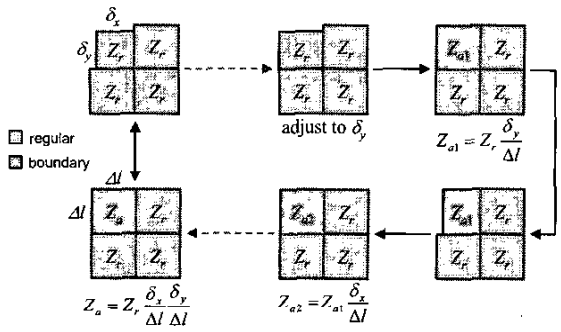

Figure 4 Modeling of a fractional cell bounded by two electric walls by means of a boundary cell. (a) A fractional cell terminated by two electric walls can be represented by a locally conformal boundary cell with impedance $Z_a = Z_r \delta_x \delta_y / (\Delta l \Delta l)$. (b) The equivalence between Z_r and Z_a is derived by two successive applications of the boundary cell theory, first in the y-direction, then in the x-direction

The example in Figure 4 contains boundary cells that represent fractional cells in one direction only. In fact, a similar adjustment can be made in the other direction as well.

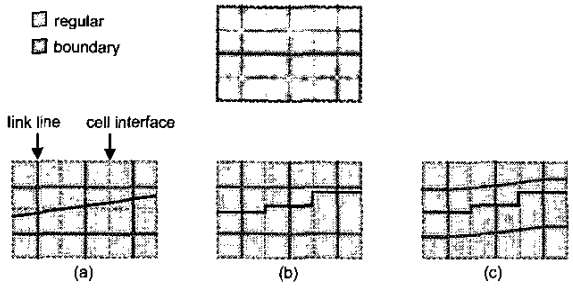

Figure 5 Replacing regular cells in a TLM mesh with boundary cells of the appropriate impedance values produces a locally conformal mesh. (a) A regular TLM mesh with a slanted boundary. (b) Ideally, the slanted boundary should be represented by regular cells of the appropriate dimensions (bottom). However, time synchronism would not be preserved in this case. Therefore, adaptive cells having the appropriate wave impedance values (top) are used to realize the equivalent response. (c) Since all the link lines of a boundary cell have the same impedance and the equivalent response is realized via some interface scattering operations, the field values at the center of the boundary cells are those that would exist at the center of the corresponding fractional cells.

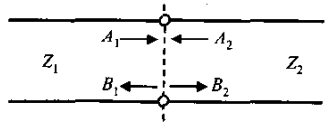

Figure 6 Connection between two boundary cells with different compression ratios.

The interface between two boundary cells must be handled properly as well because their impedance values may not be the same. Consider the situation shown in Figure 5 where two boundary cells with two different compression ratios are connected to each other. As mentioned earlier, the link lines in the boundary cells with short-circuited termination have the following properties:

$$\begin{aligned} \text{Cell 1:} \quad & Z_{x1} = Z_{y1} = Z_o \delta_1 / \Delta l \\ \text{Cell 2:} \quad & Z_{x2} = Z_{y2} = Z_o \delta_2 / \Delta l \end{aligned} \tag{13}$$

Therefore, one must implemented a scattering procedure at the interface between the two boundary cells as follows, Figure 6:

$$\begin{bmatrix} B_1 \\ B_2 \end{bmatrix} = \begin{bmatrix} \frac{n-1}{n+1} & \frac{2}{n+1} \\ \frac{2n}{n+1} & \frac{n-1}{n+1} \end{bmatrix} \begin{bmatrix} A_1 \\ A_2 \end{bmatrix} \quad \text{where} \quad n = \frac{\delta_2}{\delta_1} \tag{14}$$

In general, when the adjacent adaptive cells are associated with different compression ratios in both directions, then the ratio is: $n = (\delta_{2x} \delta_{2y}) / (\delta_{1x} \delta_{1y})$.

VALIDATION

The theory of the conformal boundary cell is validated in this section by two simulation examples. The TM and TE mode cutoff frequencies of the WR28 waveguide are obtained with the regular TLM cell and the locally conformal TLM cell, respectively. The result is tabulated in Table 1. The TM mode response is plotted in Figure 7.

As a second example, the TM and TE mode cutoff frequencies of a circular waveguide (23 cm diameter) are obtained with the regular cell and locally conformal cells, respectively. The results are shown in Table 2. The TM mode response is plotted in Figure 8. The data in Table 2 show that all the TE mode results obtained with the conformal cell are better than those obtained with the regular cell. For the TM cases, the boundary cell does not always give better results than the regular cell; however, the errors are of the same order of magnitude as those of the regular cell.

	Mode	TE10	TE20/01	TE11	TE21	TM11	TM21
	Theoretical [GHz]	21.08	42.16	42.16	59.63	47.13	59.61
Δl = 0.015 in	Regular [GHz]	20.70	41.36	48.31	60.14	48.31	60.21
	Difference [%]	1.80	1.87	2.50	0.89	2.50	1.01
	Conformal [GHz]	21.08	42.02	47.18	59.67	47.23	59.72
	Difference [%]	0.00	0.31	0.11	0.10	0.21	0.18
Δl = 0.0075 in	Regular [GHz]	21.27	41.55	46.53	59.39	46.56	59.33
	Difference [%]	0.90	1.42	1.27	0.37	1.21	0.47
	Conformal [GHz]	21.08	42.11	47.09	59.58	47.08	59.62
	Difference [%]	0.00	0.09	0.08	0.05	0.11	0.02

Table 1: The TE and TM mode cutoff frequencies obtained with the regular and locally conformal TLM cells.

	Mode	TE11	TE21	TE01	TE31	TM01	TM11
	Theoretical [GHz]	0.764	1.267	1.600	1.743	0.998	1.600
Δl = 1.0 cm	Regular [GHz]	0.751	1.224	1.577	1.682	0.997	1.586
	Difference [%]	1.702	3.394	1.438	3.500	0.100	0.875
	Conformal [GHz]	0.759	1.238	1.592	1.708	1.002	1.595
	Difference [%]	0.615	2.289	0.500	2.008	0.421	0.313
Δl = 0.5 cm	Regular [GHz]	0.760	1.248	1.588	1.719	1.000	1.592
	Difference [%]	0.563	1.500	0.750	1.377	0.190	0.500
	Conformal [GHz]	0.760	1.251	1.588	1.721	0.999	1.590
	Difference [%]	0.524	1.263	0.750	1.262	0.080	0.625

Table 2: The TE and TM mode cutoff frequencies of a circular waveguide (diameter = 23cm). The discrepancies for the TM modes are due to insufficiently resolved high spatial field variation close to the center of the waveguide rather than to inaccurate boundary position.

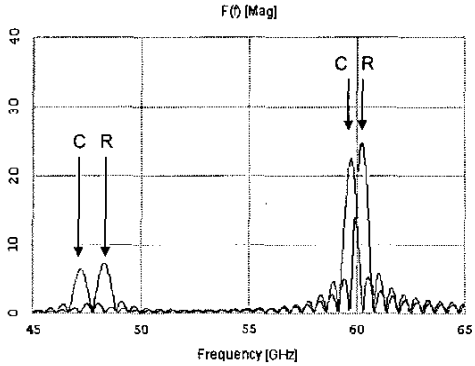

Figure 7 TM mode cutoff frequencies of a WR28 waveguide. The R and C curves are computed using regular and conformal cells, respectively. $\Delta l = 0.015$".

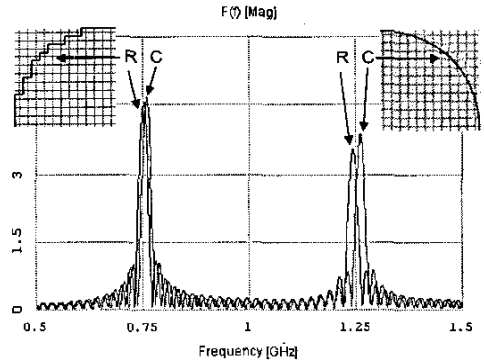

Figure 8 TE mode cutoff frequencies of a 23 cm circular waveguide. The R and C curves are computed using regular and conformal cells, respectively. $\Delta l = 1.0$ cm. The inserts on the top depict the boundaries of a regular mesh and a conformal mesh.

CONCLUSION

A locally conformal TLM cell and mesh have been presented in this paper. The feature has been integrated into a meshing algorithm for the TLM discretization of structures. The algorithm provides an unprecedented modeling capability, without imposing a time step smaller than the global TLM time step. Simulation examples have been used to validate the theory and implementation. The results show that, when the structure to be analyzed involves only straight line boundaries parallel to the mesh axes, the locally conformal mesh always yields more accurate results than the regular mesh.

REFERENCES

[1] P.B. Johns, *Transient Analysis of Waveguides with Curved Boundaries,* Electron Letter, vol. 9, no. 21, October 1973.

[2] U. Mueller, A Beyer and W.J.R. Hoefer, *Moving Boundaries in 2D and 3D TLM Simulations Realized by Recursive Formulas,* IEEE Trans. on Microwave Theory and Techniques, vol. 40, no. 12, December 1992.

[3] J.L. Herring and C. Christopoulos, *Solving Electromagnetic Field Problems using a Multiple Grid Transmission Line Modeling Method,* IEEE Trans. on Antennas and Propagation, vol. 42, vol. 12, p.p. 1654–1658, December 1994.

[4] J.L. Herring and C. Christopoulos, *The Use of Graded and Multigrid Techniques in Transmission Line Modeling, Second International on* Computation in Electromagnetics, p.p. 142–145, 1994.

[5] J. Ritter and F. Arndt, *A Generalized 3D Subgrid Technique for the Finite-Difference Time Domain Method,* IEEE MTTS Digest, p.p. 1563–1566, June 1997.

[6] R. Lotz, J Ritter and F. Arndt, *3D Subgrid Technique for the Finite Difference Method in the Frequency Domain,* IEEE MTTS Digest, p.p. 1793–1796, June 1998.

[7] G. Marrocco, M Sabbadini and F. Bardati, *FDTD Improvement by Dielectric Subgrid Resolution,* IEEE Trans. on Microwave Theory and Technique, vol. 46, no. 12, p.p. 2166–2169, December 1998.

[8] M. White, Z. Yun and M. Iskander, *A New 3D FDTD Multigrid Technique with Dielectric Traverse Capabilities,* IEEE Trans on Microwave Theory and Techniques, vol. 49, no. 3, p.p. 422–430, March 2001.

[9] S. Georgakopoulos, R. Renaut, C. Balanis and C. Birtcher, *A Hybrid Fourth-Order FDTD Utilizing a Second-Order FDTD Subgrid,* IEEE Microwave and Wireless Components Letters, vol. 11, no. 11, p.p. 462–464, November 2001.